Theory for Establishing Proximity Relations in Biological Membranes by Excitation Energy Transfer Measurements

Juan Yguerabide
Department of Biology, University of California, San Diego, La Jolla, California 92093 USA

ABSTRACT In a previous publication (Shaklai et al., 1977a) the present author developed a theory for evaluating proximity relations and surface densities σ in biological membranes by measurements of excitation energy transfer from a donor attached to a specific site of a membrane protein and an acceptor attached to a specific carbon on a membrane lipid. It was assumed that the protein and lipid are randomly distributed in the plane of the membrane and that the donor and acceptor groups are confined to different planes in the membrane separated by a distance R_p. In this article several aspects of the theory presented in the previous paper are clarified, especially noting that the previous theoretical expressions for the time-dependent and steady state fluorescence intensities assumed that the labeled protein molecule is cylindrically symmetric with the symmetry axis perpendicular to the plane of the membrane and that the donor is positioned on the symmetry axis of the protein. This assumption is also implicitly or explicitly made in subsequent formulations by other investigators. In this article we generalize the theory to include the case where the donor is not on the symmetry axis of the labeled protein. Equations for calculating the time-dependent and steady state fluorescence intensities for this more general case are presented, and methods for applying these theoretical expressions to the analysis of steady state fluorescence intensity data and evaluation of proximity parameters are discussed. It is also shown in this article that the linear relation $I/I_0 = 1 + Kq\sigma$ previously derived for simple analysis of excitation transfer data for the condition r_c/R_0 1 can be modified to apply to almost all practical ranges of r_c/R_0 without much affecting its simplicity in the analysis of experimental data.

INTRODUCTION

Several years ago, the present author developed a theory for establishing proximity relations in biological membranes by fluorescence intensity measurements of dipole-dipole excitation energy transfer between appropriately positioned donor and acceptor groups, and together with Shaklai and Ranney used this theory to characterize experimentally the interactions of hemoglobin with the red cell membrane (Shaklai et al., 1977a, b). The theory was developed for donor and acceptor groups that, in general, are each randomly distributed in separate (or same) planes parallel to the membrane surface as exemplified in Fig. 1. In this figure the donor is attached to a specific site on a membrane protein, and the acceptor is covalently attached to a specific site on a membrane lipid. The lipid and protein are assumed to be randomly distributed in their longitudinal planes. The donor could equally well be on the lipid and the acceptor on the protein without affecting the theory.

The theoretical expressions that were derived in Shaklai et al. (1977a) allow the distance between the donor and acceptor groups to be evaluated from experimental measurements of the fluorescence intensity of the donor at different acceptor concentrations (surface densities) in the membrane. More specifically, one can evaluate the closest distance r_c to which acceptor molecules can approach a donor molecule in the membrane. This distance of closest approach is determined by geometrical factors related to the size and membrane positions of the labeled membrane protein and lipid and, thus, gives information on these important parameters. The theory also allows the surface density of acceptors to be determined by fluorescence intensity measurements with a donor-labeled lipid.

The general theory developed in Shaklai et al. (1977a) relates fluorescence intensity I of the donor to r_c and surface density σ of the acceptor through an integral expression. However, for the case r_c R_0 (where R_0 is the distance between donor and acceptor at which transfer efficiency is 50%), it was shown that the fluorescence intensity can be described by the simple linear relation $I_0/I = 1 + Kq\sigma$ where Kq depends on r_c/R_0 (see Eqs. 15–17 in the present text). This relation greatly simplifies the analysis of experimental data. It allows r_c to be simply determined from the slope of a plot of I_0/I vs. σ. It can also be used to determine experimentally the surface density σ of acceptor (using a donor-labeled lipid incorporated into the membrane and a value for Kq). The latter capability allows one to determine, for example, membrane binding affinities of donor-labeled proteins as we demonstrated for hemoglobin binding to the red cell membrane using a donor-labeled fatty acid (Shaklai et al., 1977a, b).

Other investigators have examined various aspects of our original theoretical formulation, especially to derive analytical relations for fluorescence intensity vs. σ that apply in different ranges of r_c/R_0. Fung and Stryer (1978) investigated the effects of membrane curvature, which is important for lipid vesicles with very small diameters, and further tested

Received for publication 23 September 1993 and in final form 21 December 1993.

Address reprint requests to Juan Yguerabide, Department of Biology, University of California, La Jolla, CA 92093. Tel: 619-534-2455; Fax: 619-459-0635.

0006-3495/94/03/683/11 $2.00

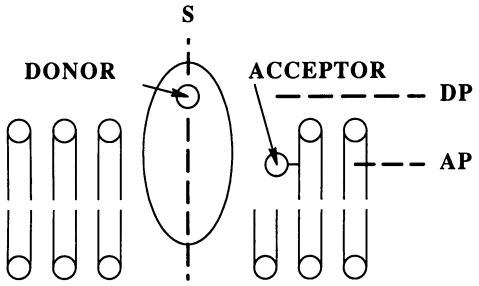

FIGURE 1 Schematic representation of the membrane excitation energy transfer model in which excitation energy transfer groups are confined to the plane DP and the acceptor groups to the plane AP. The planes DP and AP are parallel to the membrane surface. The model is exemplified here with the donor attached to a protein molecule (*ellipse*) and the acceptor to a lipid molecule. Although only one donor and one acceptor group are shown, many acceptors are assumed to be randomly distributed in the AP plane around the donor.

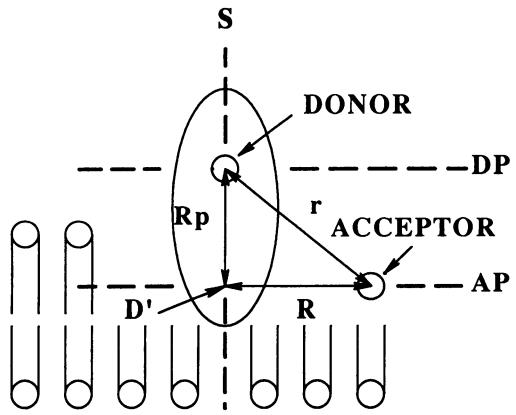

FIGURE 2 On-axis excitation energy transfer model in which the donor D is positioned at a specific point on the symmetry axis S of a cylindrically symmetric protein and the acceptor A is attached to a lipid (the lipid attachment is not shown in the figure). The symmetry axis is perpendicular to the membrane surface, and DP and AP are the planes, respectively, in which the donor and acceptor groups are confined. R_p is the perpendicular distance between the donor and acceptor planes. r is the distance between D and a given acceptor group A. R is the distance between D′ and A where D′ is the perpendicular projection of D onto the acceptor plane.

the ability of the technique to measure the surface density of donor molecules using donor- and acceptor-labeled lipids. Wolber and Hudson (1979) derived an analytical expression for I vs. σ that applies for $r_c \ll R_0$. Dewey and Hammes (1980) derived a corresponding expression that applies in the range $r_c/R_0 > 0.7$. The expressions of these investigators, however, are not as simple to use as our original linear relation. In this report, we show that our linear relation can be modified to apply to almost all ranges of r_c/R_0 encountered in practice without much affecting its easiness of use. More specifically, we present the modified relation $I/I_0 = 1 + \gamma Kq\sigma$, where γ is a factor that depends r_c/R_0, and show how to use it in practice.

We also note in this report that our original formulation, as well as other formulation that have followed, implicitly assumed that the donor (or acceptor) is positioned along the symmetry axis of the labeled protein (see Figs. 1 and 2 in this report). This assumption is especially problematic when, for example, the donor (or acceptor)-labeled protein penetrates into the plane of the acceptor (or donor) as explained in a later section. In our studies of hemoglobin this was not a problem because the donor hemoglobin molecule was not expected to penetrate into the acceptor plane. In this article we generalize our original formulation to now cover the case where the acceptor (or donor) on a labeled protein is not on the symmetry axis of the protein and discuss how to apply the new formulation to experimental results. In an accompanying article, we apply this new formulation to establish proximity relations in the membrane-associated acetylcholine receptor.

Other pertinent publications are Baird et al. (1979), Doody et al. (1983), Eisinger and Flores (1982), Fleming et al. (1979), Gutierrez-Merino (1981a, b), Hammes (1981), Holowka and Baird (1983a, b), Issacs et al. (1986), Koppel et al. (1979), Sklar et al. (1980), Estep and Thompson (1979), Van der Werf and Ullman (1979). Previous applications of excitation energy transfer in membranes are Cantley and Hammes (1976), Tweet et al. (1964), Vanderkooi et al. (1977), and Veatch and Stryer (1977).

THEORY

Theoretical model

To reduce the abstractness of the theoretical presentation, it is convenient to discuss the theory in terms of specific models. Some specific models of interest are: (1) the donor and acceptor groups are confined to the same lipid monolayer of the membrane, and there are no donor or acceptor groups in the other monolayer; (2) the donor groups are confined to one monolayer of the membrane and the acceptor groups to the other monolayer; (3) both monolayers contain donor and acceptor groups, but the donors in each monolayer interact only with acceptors in that monolayer; and (4) both monolayers contain donor and acceptor groups, and the donor group in one monolayer interacts with acceptor groups in both monolayers. For simplicity, we will present the theory in terms of a model in which the *donor and acceptor groups are randomly distributed in different planes in the same monolayer* of the membrane as exemplified in Fig. 1 and that the other monolayer does not contain any donor and acceptor groups. However, as discussed in the last section of this article, the expressions derived with this model actually apply to cases 1–3 above and can easily be generalized to apply to case 4 as well as other cases not listed here. The theory also applies when the donor and acceptor groups are in the same plane. Furthermore, although the expressions that are derived in the following sections are written with the donor attached to a protein and the acceptor attached to a lipid, the donor and acceptor groups can actually be interchanged in these expressions, that is, *the expressions also apply when the donor is on the lipid and the acceptor is on the protein or both on lipids. They also apply when the donor and acceptor are both on proteins.* We will assume that the *protein has cylindrical symmetry about an axis perpendicular to the membrane.* The

assumption that the donor and acceptor groups are confined to specific planes is not strictly correct because bending and rotational motions of the lipid and protein change the verticle positions of the donor and acceptor groups relative to the membrane surface. However, the assumption is acceptable within the other assumptions of the theory. It is also assumed that: (1) donor and acceptor molecules do not move laterally during the lifetime of the donor, and (2) the density of the excited donor molecules produced by the light beam is exceedingly small compared to the density of the acceptor molecules. The latter assumption allows one to derive all the necessary expressions from a consideration of the interactions of one single excited donor molecule with the acceptor molecules in its vicinity.

If the donor-labeled protein penetrates into the acceptor plane, then the distance of closest approach is determined not only by the perpendicular distance R_p between the donor and acceptor planes but also by the size of the donor-labeled protein and acceptor-labeled lipid (or protein) molecules (see Fig. 2). The simplest case to treat theoretically is the one in which the donor is positioned at a specific point on the symmetry axis of the protein (On-Axis case). A more general case is one in which the donor is positioned at a site not on the symmetry axis (Off-Axis case). These two cases are treated in this paper.

Donor is positioned on the symmetry axis of a cylindrically symmetric protein: On-Axis model

Fig. 2 exemplifies the case in which the donor group is positioned at a specific point on the symmetry axis and also shows the coordinate system that we will use to describe proximity relations between donor and acceptor groups in the membrane. R_p is the perpendicular distance between the planes in which the donor and acceptor groups reside. r is the distance between a given acceptor group A and a given donor group D in the membrane, and R is the distance between these groups projected onto the plane of the acceptor groups. These three distances are related by the expression

$$r^2 = R^2 + R_p^2 \tag{1}$$

The value of R has a lower limit or minimal value that is the distance of closest approach in the plane of the acceptor. As mentioned, this value is determined by geometrical factors that include the size of the protein and lipid to which the donor and acceptor groups are attached. We designate this distance of closest approach in the acceptor plane by the symbol R_c. The distance of closest approach can also be expressed in terms of the distance r, which we designate as r_c. R_c and r_c are related by the expression

$$r_c^2 = R_c^2 + R_p^2 \tag{2}$$

All distances are in cm unless stated otherwise.

Consider now a cuvette containing a membrane suspension with donor and acceptor groups incorporated in the membrane in a manner that satisfies the model being considered here. If the donor is excited by a fast pulse of light, as shown in Shaklai et al. (1977a), then the decay of fluorescence intensity is given by

$$I(t) = I(0)e^{-t/\tau_0}e^{-\sigma M(t)} \tag{3}$$

where t is time in s, τ_0 is the lifetime of excited D in s in the absence of acceptor, σ is the density of acceptor molecules in the membrane in units of molecules per cm^2, and $M(t)$ is given by

$$M(t) = \int_{r_c}^{\infty} (1 - e^{-k(r)t})2\pi r\, dr \tag{4}$$

$M(t)$ has units of cm^2. $k(\Omega, r) \equiv k(r)$ is the specific rate for dipole-dipole excitation transfer from a donor to an acceptor group separated by the distance r and according to Forster is given by the expression

$$k(\Omega, r) = \frac{1}{\tau_0}\left(\frac{R_0}{r}\right)^6 \tag{5}$$

where Ω refers to the orientations of the donor emission and acceptor dipole absorption moments. $k(\Omega, r)$ has units of s^{-1}. τ_0 is related to fundamental kinetic parameters by the expression

$$\frac{1}{\tau_0} = k_e + k_I \tag{6}$$

where k_e is the specific rate of emission and k_I is the specific rate for all other deactivating process of excited donor molecules in absence of the acceptor. R_0 (in angstrom units) is given by

$$R_0 = (8.7 \times 10^{23} J\kappa^2 k_e \tau 0 n^{-4})^{1/6} \tag{7}$$

where n is the refractive index of the medium between the donor and acceptor groups. Note that the value for R_0 calculated with Eq. 7 must be converted to cm when used in Eq. 5. The overlap integral J is defined by the expression

$$J = \frac{\int F_D(\lambda)\epsilon_A(\lambda)\lambda^4\, d\lambda}{\int F_D(\lambda)\, d\lambda} \tag{8}$$

where $F_D(\lambda)$ is the relative intensity in the emission spectrum of the donor (plotted as photons versus wavelength in cm), $\epsilon_A(\lambda)$ is the molar decadic extinction coefficient in M^{-1} cm^{-1}, and λ is wavelength in cm. J has units of cm^6 mmole^{-1}. κ is an orientation factor that depends on the orientations, Ω, of the emission and absorption moments of the donor and acceptor groups, respectively, and is defined by the expression

$$\kappa = \cos\theta_{DA} - \cos\theta_D\cos\theta_A \tag{9}$$

where θ_{DA} is the angle between the donor emission and acceptor absorption moments, θ_D is the angle between the donor emission and the line ℓ joining the donor and acceptor groups, and θ_A is the angle between the acceptor and the line ℓ. As indicated by the above expressions, at any distance r, the rate of excitation transfer depends not only on r but also

on the relative orientations of the donor emission and acceptor absorption moments. Here we will assume for simplicity that κ is the same for all donor-acceptor pairs in the membrane.

The steady state donor fluorescence intensity I for the donor-acceptor systems described in the preceding sections is in general related to $I(t)$ by the expression

$$I = a \int_0^\infty I(t)\, dt \tag{10}$$

where a is a constant of proportionality.

In order to obtain explicit analytical expressions for $I(t)$ and the steady state intensity I of Eqs. 3 and 10, respectively, it is necessary first to integrate Eq. 4. As indicated in Shaklai et al. (1977a), the integral of Eq. 4 cannot be evaluated analytically in general. However, in the special case where r_c R_0 it is shown in Shaklai et al. (1977a) that the integration can be done analytically (by power series expansion of exp-$[-(k(r)t)]$ in Eq. 4 and retention of the first two terms of the expansion) and the integration yields

$$M(t) = \frac{\pi R_0^2}{2\tau_0}\left(\frac{R_0}{r_c}\right)^4 t \tag{11}$$

Introducing Eq. 11 into Eq. 3 we get

$$I(t) = I(0)\exp - \left(\frac{1}{\tau_0} + k_q\sigma\right)t \tag{12}$$

where

$$k_q = \frac{\pi R_0^2}{2\tau_0}\left(\frac{R_0}{r_c}\right)^4 \tag{13}$$

k_q has units of cm^2/s. Recall that σ has units of molecules/cm^2. Introducing Eq. 12 into Eq. 10 and integrating gives the following expression for the steady state fluorescence intensity

$$I = \frac{a}{1 + K_q\sigma} \tag{14}$$

which can be rearranged to the form

$$\frac{I_0}{I} = 1 + K_q\sigma \tag{15}$$

where

$$K_q = \tau_0 k_q \tag{16}$$

$$= \frac{\pi R_0^2}{2}\left(\frac{R_0}{r_c}\right)^4 \tag{17}$$

I_0 is in the steady state fluorescence intensity in the absence of acceptor ($\sigma = 0$), and K_q is the steady state quenching constant. K_q has units of reciprocal density (cm^2/molecule). Note that Eq. 15 has the form of the Stern-Volmer equation.

The above expressions can be used to evaluate r_c from experimental measurements of donor steady state fluorescence intensity at different acceptor densities σ. If r_c R_0, the evaluation can be easily done with Eq. 15. According to Eq. 15, the slope of an experimental plot of I_0/I vs. σ gives the value of K_q. r_c can thus be evaluated from the value of the slope and Eq. 17 using the appropriate value for R_0. This was the method used in Shaklai et al. (1977a) to determine the distance of the heme groups of hemoglobin from the membrane surface where the condition $r_c > R_0$ almost prevails. However, when the condition r_c R_0 does not apply, Eqs. 4 and 10 may have to be integrated numerically to obtain plots of I_0/I vs. σ for different values of r_c. These plots can then be compared with the experimental plots to determine which value of r_c best fits the experimental plot.

To avoid numerical integrations, other investigators have since developed analytical expressions that apply to ranges other than r_c/R_0 1. Thus, Wolber and Hudson (1979) have derived an expression for I/I_0 vs. σ that applies for the case $r_c/R_0 \ll 1$. It should be noted that I/I_0 vs. σ becomes somewhat insensitive to r_c when $r_c/R_0 \ll 1$ and the expression of Wolber and Hudson contains R_0 but not r_c. Dewey and Hammes (1980) have used a rapid power series expansion in Eq. 4 to obtain approximant expressions for I_0/I vs σR_0^2, which apply over the range $r_c/R_0 \geq 0.67$. The latter expressions, however, are not as easy to use as Eq. 15. In the following paragraphs we show that the range of applicability of Eq. 15 can be extended to cover most practical ranges of r_c/R_0 without much affecting the simplicity of its use in the analysis of experimental data.

To develop a method that increases the range of applicability of Eq. 15, we first consider the nature of the deviations of plots of I_0/I vs σ calculated with Eq. 15 from the correct plots calculated by numerical integration of Eq. 4 for different values of r_c/R_0. The deviations can be most readily seen by comparing plots of I_0/I vs $\sigma R_0^2(\pi/2)(R_0/r_c)^4$ for different values of r_c/R_0 calculated with Eqs. 15–17 with those calculated with Eqs. 3, 4, and 10 by numerical integration. According to Eqs. 15–17, a plot I_0/I vs $\sigma R_0^2(\pi/2)(R_0/r_c)^4$ is a straight line with slope equal to 1 for all values of r_c/R_0. The correct plots obtained by numerical integration are shown in Fig. 3 for values of r_c/R_0 in the range 0.5–2. Several important points are revealed by Fig. 3. First, the correct plot for $r_c/R_0 = 2$ coincides with the plot of Eq. 15 (straight line with slope of 1) as expected for r_c R_0. However, for r_c/R_0 < 1.7, the correct plots do not coincide with the plot of Eq. 15 and depend on the value of r_c/R_0. Second, the plots for $r_c/R_0 < 1.7$ are not straight lines. However, for any value of $r_c/R_0 < 1.7$, the deviations from straight lines are not very large for values of I_0/I in the range 1 to at least 1.8. Furthermore, the deviations from a straight line are within the experimental errors or noise that is usually present in experimental plots of I_0/I vs σ. Thus, from a practical point of view we can assume that the plots of Fig. 3 are practically straight lines for all values r_c/R_0 and values I_0/I up to at least 1.8. Third, the slopes of the practical straight lines decrease

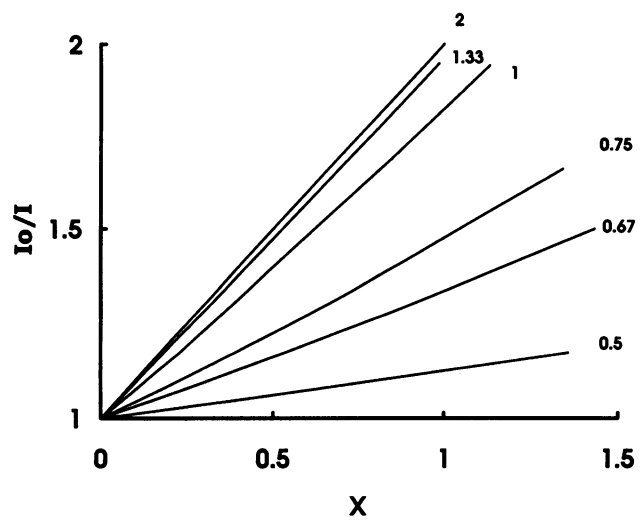

FIGURE 3 Plots of I_0/I vs. $x = \sigma R_0^2(\pi/2)(R_0/r_c)^4$ for different values of r_c/R_0 (values shown next to the plots). The plots were calculated with Eqs. 3–5 and 10 and demonstrate the deviations from the predictions of the approximate Eqs. 15–17 when r_c is not much greater than R_0.

with decreasing value of r_c/R_0. In summary, the major deviation from predictions of Eqs. 15–17 is that the slopes of the practically straight line plots of Fig. 3 are smaller than 1 when r_c is not much greater than R_0, and the slopes depend on the value of r_c/R_0.

The observation that the correct plots of Fig. 3 can be regarded as straight lines with slopes that depend on r_c/R_0 indicates that experimental plots of I vs σ can be represented, in general, by the expression

$$\frac{I_0}{I} = 1 + \gamma K_q \sigma \tag{18}$$

where K_q is still defined by Eqs. 16 and 17 and γ is a correction factor that depends on the value of r_c/R_0 (γ accounts for the dependence of slope on r_c/R_0 in Fig. 3). Table 1 gives values of γ for a several values of R_0/r_c. The values of γ were obtained from the slopes of best fitting straight lines drawn through the plots in Fig. 3 using values of I_0/I in the range 1 to ~1.7.

TABLE 1 Values of γ,* $\gamma^{1/4}$, and $r_{c,app}/R_0$ for different values of r_c/R_0

r_c/R_0	γ	$\gamma^{1/4}$	$r_{c,app}/R_0$
0.25	0.01	0.32	0.77
0.33	0.03	0.41	0.8
0.50	0.13	0.60	0.83
0.67	0.36	0.77	0.87
0.75	0.48	0.83	0.90
1	0.79	0.93	1.08
1.67	0.97	0.99	1.69
2	1	1	2

* The values for γ were calculated from the slopes of best straight lines drawn through plots of Fig. 3 (not all of the plots used to obtain Table 1 are shown in Fig. 3). Values for $r_{c,app}/R_0$ were calculated with Eq. 19.

Consider now an experimental plot of I_0/I vs σ that can be represented by a straight line and has a slope S. If we analyze the plot with Eqs. 15–17 we can calculate an apparent r_c, which we represent as $r_{c,app}$, with the expression $r_{c,app} = R_0(\pi R_0^2/2S)^{1/4}$ (this relation is obtained by solving Eq. (17) for r_c with $Kq = S$). If we analyze the plot with the Eqs.(18), (16) and (17) we can calculate the true or correct r_c with the expression $r_c = R_0(\gamma\pi R_0^2/2S)^{1/4})$. From the ratio of these expressions for r_c and $r_{c,app}$ we can write

$$r_c = r_{c,app}\gamma^{1/4} \tag{19}$$

for the relation between r_c and $r_{c,app}$. Table 1 shows values of $r_{c,app}/R_0$ for different values of r_c/R_0 evaluated with Eq.19 and values of γ from Table 1. Because γ has a value ≤ 1, it follows that $r_c \leq r_{c,app}$. A plot of the correction factor $\gamma^{1/4}$ vs $r_{c,app}/R_0$ shows that $\gamma^{1/4}$ drops gradually from a value of 1 at $r_{c,app}/R = 2$ to 0.77 at $r_{c,app}/R_0 = 0.87$ ($r_c/R_0 = 0.67$) after which it drops much faster down to 0.32 at $r_{c,app}/R_0 = 0.77$ ($r_c/R_0 = 0.25$).

From the discussion in the preceding paragraphs, we propose the following simple procedure for evaluating the corrected r_c from experimental data for any value of r_c/R_0. Draw a straight line through the experimental plot of I_0/I vs σ and evaluate the slope S. Calculate $r_{c,app}$ using the expression $r_{c,app} = R_0(\pi R_0^2/2S)^{1/4}$ or calculate $r_{c,app}/R_0$ using the expression $r_{c,app}/R_0 = (\pi R_0^2/2S)^{1/4}$. For the calculated value of $r_{c,app}/R_0$, look up in Table 1 the corresponding value for r_c/R_0 in column 1. The correct r_c can then be calculated by multiplying the latter value for r_c/R_0 by R_0. If intermediate values of $r_{c,app}/R_0$ are needed, use the data of Table 1 to make a plot of r_c/R_0 vs $r_{c,app}/R_0$ and use this plot to find the intermediate values.

Because γ appears as a fourth root in 19, the effect of γ on r_c is not as large as expected from the value of γ. Thus, for $r_c/R_0 = 1$, $\gamma = 0.778$, $\gamma^{1/4} = 0.93$, and $r_{c,app}$ and r_c differ only by a factor of 0.93, an error $(r_c - r_{c,app})/r_c$ of 7%. However, at $r_c/R_0 = 0.667$ the factor is 0.77 for an error of about 23%, and for $r_c/R_0 = 0.333$ the factor is 0.414 for an error of about 60%. A plot of $r_{c,app}/R$ vs r_c/R_0 shows that $r_{c,app}/R_0$ decreases almost linearly with decreasing values of r_c/R_0 from 2 to about 0.8 and then becomes relatively less sensitive to the value of r_c/R_0 for $r_c/R_0 < 0.7$, as expected from the relative insensitivity of I_0/I vs σ to the value of r_c/R_0 for $r_c/R_0 \ll 1$.

It is often convenient to plot experimental data as I_0/I vs σR_0^2 instead of I_0/I vs σ. σ has values in the range 0 to 10^{13} mol/cm^2, whereas σR_0^2 has the more convenient range of 0 to ~1. The slope of a graph I_0/I vsσR_0^2 is according to Eqs. 15–17 given by the expression

$$\text{slope} = \frac{\pi}{2}\left(\frac{R_0}{r_c}\right)^4 \tag{20}$$

When the experimental data are plotted as I_0/I vs σR_0^2, proceed as follows to evaluate the true or correct value of r_c. Let S' be the slope of the experimental plot I_0/I vs σR_0^2. Calculate

$r_{c,app}$ using the expression $r_{c,app}/R_0 = (\pi/2S')^{1/4}$. Using this value find the corresponding value in Table 1 for r_c/R_0, and multiply the latter by R_0 to obtain the correct value for r_c.

The range of applicability of the simple procedure described above for analysis of experimental data depends on the experimental range of σR_0^2. The smaller the range the better the approximation. In general, if the experimental plot of I_0/I vs σ or I_0/I vs σR_0^2 can be adequately represented by a straight line (does not show curvature), within the noise in the plot, then the simple procedure gives satisfactory results. If the precision of the data and range of σR_0^2 values are such that a clear curvature is seen in the experimental plot, then a more sophisticated method of analysis may have to be used. However, even in the latter case the simple procedure can be used if the analysis is restricted to the range of values of σR_0^2 where the plot is linear.

As an example of the application of the simple method of analysis proposed above, we reanalyze the data of Shaklai et al. (1977a) where the acceptor is hemoglobin bound to the inner surface of the red cell membrane and the donor is 12-(9-anthroyl)stearic acid embedded in the outer lipid monolayer of the red cell membrane. R_0 for this donor-acceptor pair is 46 Å. The slope of the experimental plot of I_0/I vs σ yields a value for $r_{c,app}$ of 42 Å or $r_{c,app}/R_0 = 0.91$. Using this value, we find from Table 1 that $r_c/R_0 = 0.75$, and the true or correct value of r_c is $0.75 \times 46 = 34.5$ Å. It should be noted that Dewey and Hammes (1980) have also reanalyzed the data of Shaklai et al. (1977a) by their method of approximants and obtain a value for r_c of 34 Å, which agrees very well with the value obtained by our simple procedure. As another example, we analyze the data of Fung and Stryer (1978) for energy transfer between two labeled lipids in a lipid vesicle, namely *N*-(2-dimethylaminonaphthalene-5-sulfonyl)phosphatidylethanolamine as donor and *N*-eosin-*N'*-phosphatidylethanolaminothiourea as acceptor with $R_0 =$ 50 Å and $r_c \sim 10$ Å. This is an extreme example with a very small value of r_c/R_0. A plot of I_0/I vs σ of the data of Fung and Stryer can be very well represented by a straight line (in the range $I_0/I = 1$ to 2) with slope equal to 1.2×10^{-12} cm^2/molecule. From this slope and $R_0 = 50$ Å we calculate $r_{c,app}/R_0 = 0.77$. From the latter value and Table 1 we get $r_c/R_0 \sim 0.25$, from which we calculate $r_c = 12.5$ Å. This value for r_c agrees very well with the value of 10 Å given by Fung and Stryer.

The linear expression of Eq. 18 is also very useful for evaluating the binding affinity of an acceptor-labeled protein or ligand to a membrane containing an acceptor-labeled lipid, as demonstrated by Shaklai et al. (1977a) for the binding of hemoglobin to the red cell ghost membrane containing the donor 12-(9-anthroyl)stearic acid. For details see Shaklai et al. (1977a), but basically the procedure is as follows. First, measure I/I_0 for different concentrations of donor-labeled ligand or protein and a high membrane concentration where all of the donor-labeled ligand or protein added to the membrane suspension is bound to the membrane (stoichiometric conditions). From the concentrations of the labeled ligand or protein and membrane phospholipid, calculate σ for each concentration of ligand or protein (using 70 Å^2 for the area per membrane phospholipid molecule). Plot I/I_0 vs σ, and from the slope of the latter plot calculate γK_q (see Eq. 18). Next, measure I/I_0 for different concentrations of donor-labeled ligand at low membrane concentration (equilibrium conditions) where not all of the ligand is bound, and from these values of I/I_0 and the value of γK_q, calculate σ vs concentration of added ligand with Eq. 18. The values of σ give the amount of bound ligand vs concentration of ligand from which the dissociation constant can be calculated. Eq. 18 can also be used to evaluate the surface density σ of acceptor-labeled lipid in a membrane. The procedure is as follows. Add a small amount of donor-labeled lipid to the membrane and measure I/I_0. Calculate K_q using the appropriate R_0 value for the donor and acceptor pair used in the experiment and $r_c = 10$ Å. Calculate σ with Eq. 18 using $\gamma = 0.01$.

Finally, it should be noted that the experiments and analysis described above yield values of r_c , but not of R_p and R_c (see Eq. 2 and Fig. 2). Some of the derivations in the literature, for example Wolber and Hudson (1979), assume that when the donor group is in a different plane than the acceptor group, r_c is equal to the distance between the planes. As already noted this not true for acceptor-labeled proteins that penetrate into the acceptor plane as shown in Fig. 2. It is also untrue if the head group of the acceptor (or donor)-labeled lipid is obstructed by the bulk of the protein in the polar head region of the membrane. In general, from the value of r_c alone, we can only state that the donor is somewhere on the surface of a sphere of radius r_c centered on any chosen point in the acceptor plane. More precise localization of the donor group requires values of R_p and R_c. In principle, values for these parameters can be obtained by evaluating r_c for the acceptor positioned at two different depths in the membrane by attaching the acceptor to different carbons on the hydrocarbon chain of a lipid. The theory of this method will be presented elsewhere. In some cases it might be possible to assign a value to R_p from other considerations and calculate R_c with Eq. 2 or vice versa. Thus, in the case of hemoglobin bound to the red cell, R_c was assigned a value of zero based on physical considerations. In the latter case $r_c = R_p$.

Donor is not positioned on the symmetry axis of the cylindrically symmetric membrane protein: Off-Axis model

Fig. 4 exemplifies the case where the donor is off axis. The figure shows a cross section of the membrane taken through a plane that contains the symmetry axis of the protein and the point at which the donor is located. The position of the donor is given in this plane by the perpendicular distance δ from the symmetry axis and the perpendicular distance R_p of the donor from the plane of the acceptor. Because of the off-axis position of the donor, the distance of closest approach depends on the direction from which the acceptor approaches the donor-labeled protein. In this case, Eq. 4 does not apply because the equation assumes that r_c is independent of di-

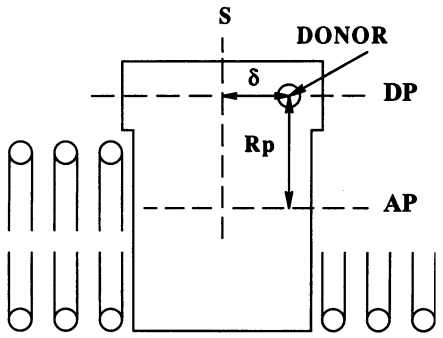

FIGURE 4 Schematic representation of the Off-Axis membrane excitation energy transfer model in which the donor D is positioned at a point that is not on the symmetry axis S of the labeled, cylindrically symmetric protein. The protein here is depicted as transversing the lipid bilayer. DP and AP are respectively the planes in which the donor and acceptor groups are randomly positioned. δ is the perpendicular distance (displacement) of D from the symmetry axis of the protein, and R_p is the distance between the donor and acceptor planes.

rection. To derive the appropriate equation for the Off-Axis case, we introduce the coordinate system of Fig. 5 *a*, which is drawn in the plane AP of the acceptor. The circle shown in Fig. 5 *a* represents the distance of closest approach to the center of the circle in the acceptor plane and has a radius α. The center of the circle is located at the point where the symmetry axis of the protein intercepts the acceptor plane. The point D′ is the perpendicular projection of the position D of the donor onto the acceptor plane as shown in Fig. 4, and δ is the distance (displacement) of D′ from the center of the circle. We describe the angular position of any acceptor group A by means of the angle θ, which is defined as the angle between the lines CD′ and D′A in Fig. 5. The distance in the acceptor plane between a give donor and acceptor is specified by R, which is the distance between the points D′ and A. The distance of closest approach of an acceptor to the point D′ in the acceptor plane is described by $R_c(\theta)$, which depends on θ. An acceptor positioned at $R_c(\theta)$ has a distance α from the center of the circle. Finally, we define $r_c(\theta)$, not shown in Fig. 5, as the distance from the donor positioned at D (see Fig. 4) to the acceptor positioned at $R_c(\theta)$.

Using the coordinate system described above, it can be shown that for the present Off-Axis case, the time-dependent and steady state fluorescence intensities are given by Eqs. 3 and 10, but $M(t)$ is now given by the expression

$$M(t) = 2\int_0^{\pi}\int_{R_c(\theta)}^{\infty}(1 - e^{-k(r)t})R\,d\theta\,dR \qquad (21)$$

which includes an integration over the angle θ. It should be noted that the lower limit of integration $R_c(\theta)$ depends on θ. To integrate Eq. 21, we must insert the expression for $k(r)$ (Eq. 5) into Eq. 21. However, the r that appears in Eq. 5 is the distance from the donor to a given acceptor, whereas the R in the integrand of Eq. 21 is the distance between the donor and acceptor measured from D′ as shown in Fig. 5. To integrate Eq. 21 we must have a relation between r and R. This relation is provided by the following

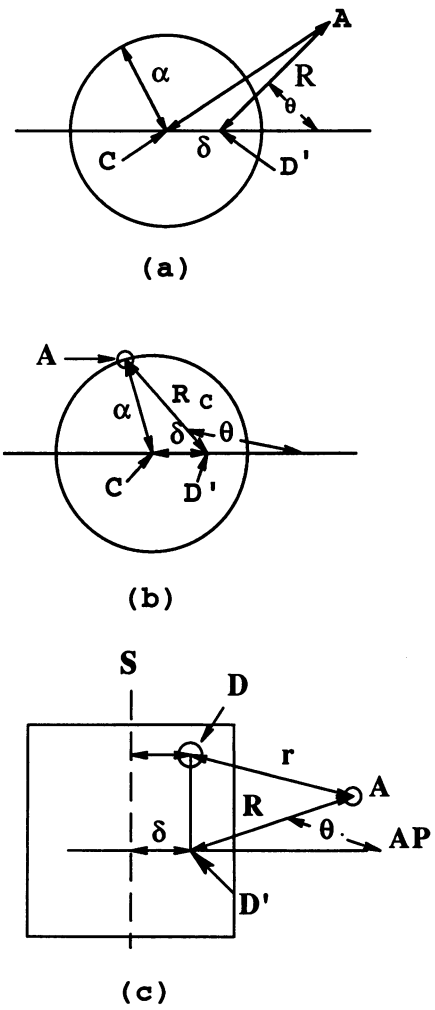

FIGURE 5 Schematic representation of the coordinate system used in the acceptor plane AP to describe the position of an acceptor group relative to the donor group in the Off-Axis membrane excitation energy transfer model. (*a*) and (*b*) are drawn completely in the acceptor plane. The radius α of the circles in (*a*) and (*b*) is the distance of closest approach of an acceptor A to center of the circle C. The center is the point where the transverse symmetry axis S of the cylindrically symmetric protein intercepts the acceptor plane. D′ is the transverse projection of the point D (position of donor) onto the acceptor plane as shown in Figs. 4 and 5 *c*. δ is the distance of the point D from the symmetry axis S or the distance of D′ from the center of the circle. (*a*) The position of A with respect to D′ in the acceptor plane is described by the distance R and angle θ. θ is the angle between the lines CD′ and D′A. (*b*) Coordinate system that is used to establish the relations shown in Eqs. 25–29. The coordinate system is the same as in (*a*) except that the acceptor is on the circle of radius α, distance of closest approach with respect to the center of the circle, at the angle θ. R_c is the distance of closest approach to the point D′ in the acceptor plane and depends on θ. (*c*) Coordinate system that is used to define the distance r from the donor D to the acceptor A. The lines D′–AP and D′–A are in the acceptor plane. R is the distance between D′ and A as in (*a*) and (*b*). The periphery of the protein defines a circle where protein intercepts the acceptor plane. The circle has a radius β equal to the longitudinal radius of the protein at the level of the acceptor plane. In general, the value of α is greater than or equal to the value of β because the value of α is influenced not only by the size of the protein but also by the dimensions of the acceptor-labeled lipid and other steric and repulsive factors.

expressions

$$r^2 = R_p^2 + R^2 \tag{22}$$

$$rdr = RdR \tag{23}$$

From the above three equations we can write

$$M(t) = 2\int_0^{\pi}\int_{r_c(\theta)}^{\infty}(1 - e^{-k(r)t})r\,d\theta\,dr \tag{24}$$

where

$$r_c(\theta)^2 = R_p^2 + R_c^2(\theta) \tag{25}$$

Finally, to perform the integration of Eq. 24 we must have a relation that shows explicitly how $r_c(\theta)$ depends on θ in terms of the fundamental proximity parameters R_p, α, and δ. We can obtain this relation from Fig. 5 *b*. From the geometry shown in Fig. 5 *b* and the law of cosines for oblique triangles we can write

$$\alpha^2 = \delta^2 + R_c(\theta)^2 - 2\delta R_c(\theta)\cos(180 - \theta) \tag{26}$$

$$= \delta^2 + R_c(\theta)^2 + 2\delta R_c(\theta)\cos(\theta) \tag{27}$$

Rearranging Eq. 27 we get

$$R_c(\theta)^2 + 2\delta R_c(\theta)\cos\theta + (\delta^2 - \alpha^2) = 0 \tag{28}$$

The above equation is a quadratic equation and has the solution

$$R_c(\theta) = -\delta\cos\theta + \sqrt{\delta^2\cos^2\theta + (\alpha^2 - \delta^2)} \tag{29}$$

Inserting Eq. 29 into Eq. 25 gives the equation that relates $r_c(\theta)$ to θ in terms of the the fundamental proximity parameter R_p, δ, and α.

The above expressions can be used to analyze experimental data consisting of a graph of steady state fluorescence intensity I vs σR_0^2 for the case where the donor is believed or known to be Off-Axis. The analysis requires numerical integration of Eqs. 24 and 10 in order to obtain graphs of I_0/I vs σR_0^2 for comparison with experimental data. The numerical integration can be performed by the following procedure.

1. First, we assign values to R_0, α, δ, R_p, and τ_0, which are the input parameters for the integration. These values are used where required in the following steps 2 and 3.

2. We initiate the integration by integrating over r in Eq. 24. To do this we assign specific values to θ and t, which we designate as θ_i and t_k. Using the latter values we numerically evaluate the following integral using the trapezoidal or Simpson rule

$$s(t_k, \theta_i) = \int_{r_c(\theta_i)}^{\infty}(1 - e^{-k(r)t_k})r\,dr \tag{30}$$

The numerical integration can be represented by the expression

$$s(t_k, \theta_i) \cong \sum_{j=1}^{N}(1 - e^{-k(r_j)t_k})r_j\Delta r \tag{31}$$

where $r_1 = r_c(\theta_i)$ and $r_N = N\Delta r$. The value of $r_c(\theta_i)$, the value of r for the first term in the sum, is calculated with the equations (from Eqs. 25 and 29)

$$r_c(\theta_i) = \sqrt{R_p^2 + R_c^2(\theta_i)} \tag{32}$$

$$R_c(\theta_i) = -\delta\cos\theta_i + \sqrt{\delta^2\cos^2\theta_i - (\delta^2 - \alpha^2)} \tag{33}$$

For the upper limit of integration we use a value of $r_{max} = gR_0 - r_c(\theta_i)$ where the value of g is in the range 5–20. The increment Δr is equal to r_{max}/N, where N is the number of values of r used in the integration over r. N is in the range 50- 150. The calculation is usually first done with $g = 5$ and $N = 50$. The calculation is then repeated with larger values of g and N. If the results change on increasing g and N, the calculation is repeated with larger values of g and N until a stable result is obtained.

Step 2 is repeated for other values of θ_i and the same t_k to generate values of $s(t_k, \theta_i)$ in the range $\theta_i = 0$ to π, with a $\Delta\theta_i$ of, say, one degree. This procedure essentially evaluates the integral of Eq. 24 over dr.

3. We next use the values for $s(t_k, \theta_i)$ generated in step 2 to evaluate the integral numerically

$$M(t_k) = 2\int_0^{\pi} s(t_k, \theta)\,d\theta \tag{34}$$

The numerical integration procedure can be represented by the expression

$$M(t_k) \cong 2\sum_{k=1}^{m} s(t_k, \theta_i)\Delta\theta \tag{35}$$

where the limits of summation in terms of θ are $\theta_1 = 0$ and $\theta_{max} = \theta_m = \pi$. Values for m and $\Delta\theta$ are chosen as described above for N and Δr.

4. Steps 2 and 3 are repeated using different values of t_k to generate values for $M(t_k)$ at different t_k. Values of $M(t_k)$ are calculated for t_k in the time range 0 to $b\tau_0$ with $b \geq 5$ and $\Delta t = b\tau_0/n_T$. n_T is the number values of t_k at which $M(t_k)$ is calculated and is in the range 50–150.

5. The values of step 4 are next used to evaluate $I(t_k)$ with Eq. 3 for a given value of σ and the values of t_k of step 4. Because only relative intensity is of interest, we let $I(0)$ equal to any convenient value, say, the value 100.

6. Finally, using the values of $I(t_k)$ of step 5, we calculate the steady state intensity for the value of σ used in step 5 by numerical integration of Eq. 10. The numerical integration can be represented by the expression

$$I = \sum_{i=1}^{nT} I(t_k)\Delta t \tag{36}$$

where the first term in the sum, $I(t_1)$, is for $t_1 = 0$ and the last term is $t_{nT} = T_{max} = 5\tau_0$. This step gives the steady state fluorescence intensity I for the assigned value of σ.

7. We repeat steps 6 and 7 for different values of σ in the range 0 to some upper value that give values of I vs σ in the range of at least $I_0/I = 1$ to at least 2.

Fig. 6 shows graphs that demonstrate the effects of δ on a plot of I_0/I vs σR_0^2. The plots were calculated by the numerical procedure described above. There are two important features to be noted from these plots. First, δ has very significant effects on the sensitivity of I_o/I to σ. For the values of α, R_p, and R_0 used in Fig. 6, I_o/I is not very sensitive to σ when $\delta = 0$, but the sensitivity increases considerably for values of $\delta \geq 50$ Å.

It should be noted that δ can have values greater than α. This is demonstrated in Fig. 7. However, Eq. 21 does not apply as it stands when $\delta > \alpha$. The required modifications can be seen by reference to Fig. 8, which shows the appropriate geometry in the acceptor plane when $\delta > \alpha$. It can be seen from this figure that when $\delta > \alpha$ any acceptor molecule can enter the point D′, which is the projection of the position of D onto the acceptor plane. Because D′ is at a distance R_p from the donor molecule, the distance of closest approach is now $r_c = R_p$ and is independent of the angle θ (recall from Fig. 5 that θ is the angle between the line CD′ and the line D′A and the D′A drawn from D′ to a given acceptor). However, for values of $\theta > \omega$ (ω is the angle between CD′ and the line D′L, which is tangent to the circle in Fig. 8), there is an area defined by the circle in Fig. 8 where acceptor molecules are excluded by the bulk of the labeled protein and lipid. To account for this exclusion area, the integral of Eq. 21 must be broken into parts. The first part, which we call $M_1(t)$, accounts for integration in the angular range $\theta = 0$ to ω and is given by the expression

$$M_1(t) = 2\omega \int_R^\infty (1 - e^{-k(r)t})r\,dr \qquad (37)$$

Consider now a line drawn from D′ to infinity at an angle in the range $\theta = \omega$ to π. This line intersects the circle at two points. Call these two points $r_1(\theta)$ and $r_2(\theta)$. The second part of the integration $M_2(t)$ is then given by the expression

$$M_2(t) = 2\int_\omega^\pi \left(\int_0^{r_1(\theta)} (1 - e^{-k(r)t})r\,dr + \int_{r_2(\theta)}^\infty (1 - e^{-k(r)t})r\,dr \right) d\theta \qquad (38)$$

The total integral is $M(t) = M_1(t) + M_2(t)$. Further details of the case $\delta > \alpha$ will be presented in another publication.

The analysis of experimental data by the Off-Axis model can be conducted by calculating plots of I_0/I vs σR_0^2 for different values of α, δ, and R_p as described above and comparing these plots with the experimental plot for goodness of fit. However, this procedure does not yield unique values for α, δ, and R_p because there are many sets of values for these parameters that fit the experimental data equally well. Recall that in the On-Axis case, one can determine the value of r_c but cannot obtain unique values for R_c and R_p from one experimental plot of I_0/I vs σR_0^2 alone because there are many values R_c and R_p that give the same value for r_c (see Eq. 2).

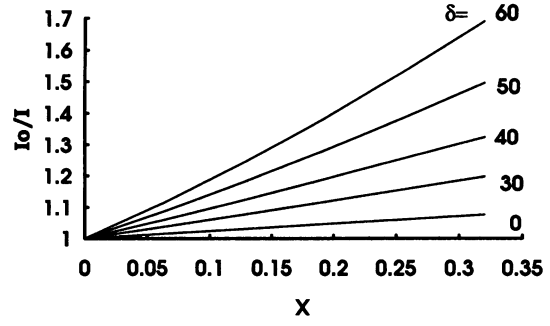

FIGURE 6 Plots of I_0/I vs. $x = \sigma R_0^2$ for the Off-Axis case demonstrating the effects of changing values of δ on this type of plots. The plots were obtained by numerical integration using Eqs. 3, 10, and 24 with $R_0 = 40$ Å, $\alpha = 60$ Å, $R_p = 20$ Å, and the values of δ shown next to each plot.

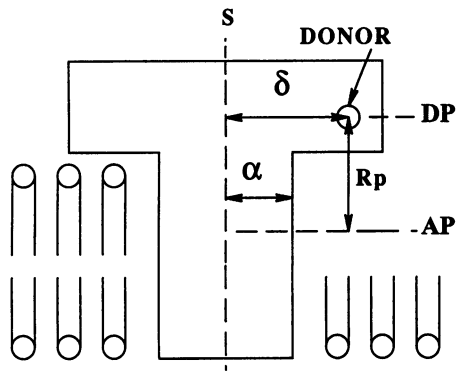

FIGURE 7 Schematic representation of a case in which δ is greater than α. The part of the protein embedded in the lipid bilayer is a thin cylinder, whereas the part of the protein in which the donor D is embedded is stretched out on the surface of the membrane. S is the symmetry axis of the cylindrically symmetric protein, and AP is the acceptor plane.

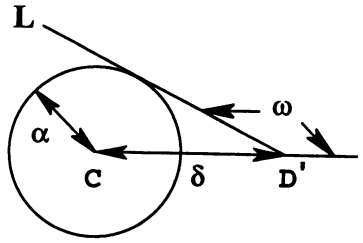

FIGURE 8 Graph showing the coordinate system used to describe the geometry in the plane of the acceptor for the case where $\delta > \alpha$. ω is the angle between the line drawn through C (point where the transverse symmetry axis of the donor-labeled protein crosses the acceptor plane) and D′ (D′ is the transverse projection of donor position onto the acceptor plane), and the line that starts at D′ and is tangent to the circle. α is the radius of the circle, and δ is the distance between C and D′ as defined in Fig. 5. The circle is an area in the acceptor plane where acceptors are excluded due to stereohinderance between the donor-labeled protein and the acceptor-labeled lipid.

In principle, α, δ, and R_p can be evaluated from measurements of I_0/I vs σR_0^2 with acceptor positioned at different depths in the membrane by attaching the acceptor to different positions on the hydrocarbon chain of a lipid molecule. The complex theory for this approach will be presented elsewhere. However, there are important applications where values for two of the three parameters α, δ, and R_p may be known from other types of experiments, in which case only one parameter is unknown. The single unknown parameter can be evaluated from a plot of I_0/I vs σR_0^2. For example, suppose that the position of the donor group in the protein and the diameter of the protein is known from other experiments and that this information can be used to assign to values to α and δ. Then the unknown parameter is R_p, which gives information on the vertical or transverse position of the protein in the membrane. In this case, the values assigned to α and δ can be used in the numerical calculation of I_0/I vs σR_0^2 for different values of R_p. The value of R_p that gives the best fit to the experimental data is the best value for R_p. This procedure is used in the accompanying article to evaluate the transverse position of the acetylcholine binding sites on its membrane-associated receptor. R_p gives the depth of the protein in terms of the transverse distance of the donor group from the acceptor plane. The transverse distance of the acceptor plane with respect to the center of the membrane is known from the known position of the acceptor on the labeled lipid. The transverse distance of the donor from the center of the membrane can then be calculated from the values of R_p and the depth of the acceptor plane.

GENERALITY OF THE THEORETICAL EXPRESSION

As indicated in the introductory sections of this article, in order to reduce the abstractness of the presentation, we have used a model in which acceptor and donor groups are located on only one of the monolayers of a biological membrane, and in which the donor is on a protein and the acceptor is on a lipid. However, the expressions presented for this model actually apply as they stand if (1) the donor is in one monolayer and the acceptor is in the other monolayer, (2) acceptor and donors are in the two monolayers, but the two monolayers are identical and donors and acceptors in different monolayers do not interact with each other, and (3) the donor is on the lipid and the acceptor on the protein. It should be noted that in Shaklai et al. (1977a) the theory was formulated in terms of the donor on the lipid and the acceptor on the protein, and the resulting expressions have the same form as, for example, Eq. 15 of this article. The model also applies if the donor and acceptor are in the same plane ($R_p = 0$).

More general cases can easily be treated by simple modifications of the expressions presented for the Off-Axis model. Consider, for example, the case where both monolayers of the membrane contain donor and acceptor molecules but the two monolayers are not identical. Then each monolayer will have its own values of α and R_p and the same value of δ. The fluorescence intensity from this system, assuming that the donor and acceptor groups in different monolayers do not interact with other, is given by the sum of two expressions of the form of Eq. 10, with one expression having the values of α_1 and R_{p1} for one monolayer and the other expression having the values of α_2 and R_{p2} for the other monolayer.

In practice the reason for using excitation energy transfer to establish proximity relations in membranes is often to determine the position of an interesting site on a membrane protein with respect to, say, the center or surface of the membrane (transverse position). To do this, a donor (or acceptor) is attached to the protein site of interest, and a lipid labeled with the acceptor (or donor) attached to a specific site on the lipid is then partitioned into the membrane. In the case of natural membranes, the membrane proteins are vectorially oriented in the membrane, and the labeled site on the protein will usually be only on one side of the membrane, that is, the donor (or acceptor) is in only one monolayer of the membrane. The labeled lipid, however, is expected to be on both monolayers, although not necessarily with equal densities, because the vectorial orientation of lipids in natural membranes is not absolute. In natural membranes we thus expect that the case that prevails in general is one in which the donor is restricted to one monolayer, the acceptor is in both monolayers, and the donor can transfer excitation energy to acceptor groups in both monolayers. In this case the fundamental equation for $I(t)$, Eq. 3, has the following modified form.

$$I(t) = I(0)\exp(-t/\tau_0 \exp\{-[\sigma_1 M_1(t) + \sigma_2 M(t)]\}) \qquad (39)$$

where subscript 1 refers to the monolayer in which the donor is positioned and subscript 2 refers to the opposite monolayer. $M_1(t)$ and $M_2(t)$ are given by Eq. 24 with $\alpha_1$and R_{p1} for $M_1(t)$ and $\alpha_2$and R_{p2} for $M_2(t)$. σ_1 and σ_2 account for the different densities of the acceptor in the two monolayers of the membrane. Equation 10 still applies. In general, the number of proximity parameters that appear in Eq. 39 makes the equation somewhat unwieldy for analysis of experimental data. However, the situation can be simplified by introducing restrictive information that can be readily obtained. For example, Rp_1 and R_{p2} are usually not independent. Because the acceptor-labeled lipid is the same in both monolayers, the position of the acceptor from the center of the membrane is known for both monolayers. This information can be used to express R_{p2} in terms of R_{p1}, thus reducing the number of fitting parameters. Moreover, if the donor is far removed from the center of the membrane, and if the acceptors are not close to the center of the membrane, it is likely that the interaction of the donor with the acceptors on the opposite monolayer can be ignored (because of the $1/r^6$ dependence of dipole-dipole excitation energy transfer (see Eq. 5). In this case, Eq. 3 can be used without modification. The conditions under which interaction with acceptors on the opposite monolayer can be ignored can be determined by simulations with Eq. 39. In general, it is best to use a labeled lipid in which the acceptor is so positioned that interactions with the opposite monolayer can be ignored.

In summary, Eqs. 3, 24, and 10 describe the time-dependent and steady state fluorescence intensities of the case where the donor is not on the symmetry axis of the cylindrically symmetric, labeled membrane protein. These equations are actually more general than the model used to derive them and apply to many other cases or can easily be modified for more general cases as discussed in the above sections. When $\delta = 0$, the Off-Axis case reduces to the On-Axis case. More specifically, when $\delta = 0$, Eq. 24 reduces to Eq. 4. Equations 3 and 10 are the same for both cases. In practice the analysis of experimental data with Eqs. 3, 24, and 10 in order to obtain values for the proximity parameters is done by comparing the experimental I_0/I vs. σR_0^2 with graphs calculated with these equations. The calculation of a theoretical plot requires assignment of values to at least five parameters, namely, τ_0, R_0, α, δ, and R_p. τ_0 and R_0 are not actually independent parameters that are to be adjusted for best fit, because the value of τ_0 is determined experimentally by lifetime measurements of the donor in the absence of acceptor and R_0 is calculated from spectroscopic data by Eq. 7. Thus, α, δ, and R_p are the three proximity parameters (assuming that the donor transfers energy to acceptors in only one plane) whose values are adjusted for best fit of the theoretical expressions to the experimental data and that yield the interesting information on how the donor label and labeled protein are positioned in the membrane. If the donor can transfer energy to acceptors in both monolayers of a membrane then there are more than three proximity parameters to be fitted as discussed for Eq. 39. It is best to set up the experiments to avoid this situation. However, even in the case where there are only three proximity parameters to be evaluated by comparison of experimental and theoretical graphs, unique values for these parameters cannot be obtained from one experimental graph alone because there are different sets of values for the parameters that fit the data equally well. This can be most clearly seen from Eqs. 15–17 for the On-Axis case, which shows that in this case one can obtain a unique value for r_c, but not unique values for R_c and R_p, because any values of R_c and R_p that satisfy the relation $r_c^2 = R_c^2 + R_p^2$ fit the data equally well. There are several ways to approach the problem of determining unique values for the fundamental proximity parameters. One is to assign values to two of the parameters from other types of experiments. This then leaves only one fitting parameter that can then be evaluated uniquely from the experimental data.

Analytical solutions for the Off-Axis case are being developed and will be presented elsewhere.

I thank Evangelina E. Yguerabide for assistance with the graphs and drawings and Dr. David A. Johnson and Dr. Jose Maria Alvarez for reading the manuscript and providing useful comments.

REFERENCES

Armstrong, S. A, E. J. Husten, C. T. Esmon, and A. E. Johnson. 1990. The active site of membrane-bound meizothrombin. A fluorescence determination of its distance from the phospholipid surface and its conformational sensitivity to calcium and factor Va. *J. Biol. Chem.* 265: 6210–6218.

Baird, B., U. Pick, and G. G. Hammes. 1979. Structural investigation of reconstituted chloroplast ATPase with fluorescence measurements, *J. Biol. Chem.* 254:3818–3825.

Cantley, L. C., and G. G. Hammes. 1976. Investigation of quercetin binding sites on chloroplast coupling factor 1. *Biochemistry.* 15:1–8.

Dewey, T. G., and G. G. Hammes. 1980. Calculation of fluorescence resonance energy transfer on surfaces. *Biophys. J.* 32:1023–1035.

Doody, M. C., L. A. Skalar, H. J. Pownall, J. T. Sparrow, A. M. Gotto, and L. C. Smith. 1983. A simplified approach to resonance energy transfer in membranes, lipoproteins, and spatially restricted systems. *Biophys. Chem.* 17:139–152.

Eisinger, J., and J. Flores. 1982. The relative locations of intramembrane fluorescent probes and the cytosol hemoglobin in erythrocytes, studied by transverse resonance energy transfer. *Biophys. J.* 37:6–7.

Estep, T. N., and T. E. Thompson. 1979. Energy transfer in lipid bilaryers. *Biophys. J.* 26:195*a*. (Abstr.).

Fernandez, S. M., and R. D. Berlin. 1976. Cell surface distribution of lectin receptors determined by resonance energy transfer. *Nature (Lond.).* 264: 411*a*. (Abstr.).

Fleming, P. J., D. E. Koppel, A. L. Y. Lau, and P. Strittmatter. 1979. Intramembrane position of the fluorescent tyrptophanyl residue in the membrane-bound cytochrome b_5. *Biochemistry.* 18:5458–5464.

Fung, B. K. K., and L. Stryer. 1978. Surface density of determination in membranes by fluorescence energy transfer. *Biochemistry.* 17:5241–5248

Gutierrez-Merino, C. 1981a. Quantitation of the Forster energy transfer for two-dimensional systems. I. Lateral phase separation in unilamellar vesicles formed by binary phospholipid mixtures. *Biophys. Chem.* 14: 247–257.

Gutierrez-Merino, C. 1981b. Quantitation of the Forster energy transfer for two-dimensional systems. II. Protein distribution and aggregation state in biological membranes. *Biophys. Chem.* 14:259–266.

Hammes, G. G. 1981. Fluorescence Methods. *In* Protein–Protein Interactions. C. Frieden and L. W. Nichol, editors. Wiley Interscience, New York. 257–287.

Holowka, D., and B. Baird. 1983a. Structural studies on the membrane-bound immunoglobulin E-receptor complex 1. Characterization of large plasma membrane vesicles from rat basophilic leukemia cells and insertion of amphipathic fluorescent probes. *Biochemistry.* 22:3466–3474.

Holowka, D., and B. Baird. 1983b. Structural studies on the membrane-bound immunoglobulin E-receptor complex 2. Mapping the distance between sites on IgE and the membrane surface. *Biochemistry.* 22:3475–3484.

Isaacs, B. S., E. J. Husten, C. T. Esmon, and A. E. Johnson. 1986. A domain of membrane-bound coagulation factor Va is located far from the phospholipid surface. A fluorescence energy transfer measurement. *Biochemistry.* 25:4958–4969.

Koppel, D. E., P. J. Fleming, and P. Strittmatter. 1979. Intramembrane positions of membrane-bound chromophores determined by excitation energy transfer. *Biochemistry.* 18:5450–5457.

Shaklai, N., J. Yguerabide, and H. M. Ranney. 1977a. Interaction of hemoglobin with red blood cell membranes as shown by a fluorescent chromophore. *Biochemistry.* 16:5585–5592.

Shaklai, N., J. Yguerabide, and H. M. Ranney, H. M. 1977b. Classification and location of hemoglobin binding sites on red blood cell membranes. *Biochemistry.* 16:5593–5597.

Sklar, L. A., M. C. Doody, A. M. Gotto, and H. J. Pownall. 1980. Serum lipoprotein structure: resonance energy transfer localization of fluorescent probes. *Biochemistry.* 19:1294–1301.

Tweet, A. G., W. D. Bellamy, and G. L. Gaines. 1964. Fluorescence quenching and energy transfer in monomolecular films containing chlorophyll. *J. Chem. Phys.* 41:2068.

Van Der Werf, P., and E. F. Ullman. 1979. Measurement of liposome fusion by energy transfer measurements. *Fed. Proc.* 38:459*a*. (Abstr.).

Vanderkooi, J. M., A. Ierokomas, H. Nakamura, and A. Martonosi. 1977. Fluorescence energy transfer between Ca^{2+} transport ATPase molecules in artificial membranes. *Biochemistry.* 16:1262–1267.

Veatch W., and L. Stryer. 1977. The dimeric nature of the Gramicidin A transmembrane channel: conductance and fluorescence energy transfer studies of hybrid channels. *J. Mol. Biol.* 113:89–102.

Wolber, P. K., and B. S. Hudson. 1979. An analytic solution to the Forster energy transfer problem in two dimensions. *Biophys. J.* 28:197–210.